

Arnold diffusion for a complete family of perturbations with two independent harmonics*

Amadeu Delshams[†] and Rodrigo G. Schaefer[‡]

Departament de Matemàtiques and Lab of Geometry and Dynamical Systems
Universitat Politècnica de Catalunya, Barcelona

November 15, 2021

To Rafael de la Llave on the occasion of his 60th birthday

Abstract

We prove that for any non-trivial perturbation depending on any two independent harmonics of a pendulum and a rotor there is global instability. The proof is based on the geometrical method and relies on the concrete computation of several scattering maps. A complete description of the different kinds of scattering maps taking place as well as the existence of piecewise smooth global scattering maps is also provided.

MSC2010 numbers: 37J40

Keywords: Arnold diffusion, Normally hyperbolic invariant manifolds, Scattering maps

1 Introduction

1.1 Main result

We consider an *a priori unstable* Hamiltonian with $2 + 1/2$ degrees of freedom

$$H_\varepsilon(p, q, I, \varphi, s) = \pm \left(\frac{p^2}{2} + \cos q - 1 \right) + \frac{I^2}{2} + \varepsilon h(q, \varphi, s) \quad (1)$$

consisting of a pendulum and a rotor plus a time periodic perturbation depending on two harmonics in the variables (φ, s) :

$$\begin{aligned} h(q, \varphi, s) &= f(q)g(\varphi, s), \\ f(q) &= \cos q, \quad g(\varphi, s) = a_1 \cos(k_1 \varphi + l_1 s) + a_2 \cos(k_2 \varphi + l_2 s), \end{aligned} \quad (2)$$

with $k_1, k_2, l_1, l_2 \in \mathbb{Z}$.

The goal of this paper is to prove that for *any* non-trivial perturbation $a_1 a_2 \neq 0$ depending on *any* two *independent* harmonics $\begin{vmatrix} k_1 & k_2 \\ l_1 & l_2 \end{vmatrix} \neq 0$, there is global instability of the action I for any $\varepsilon > 0$ small enough.

*This work has been partially supported by the Spanish MINECO-FEDER grant MTM2015-65715 and the Catalan grant 2014SGR504. AD has been also partially supported by the Russian Scientific Foundation grant 14-41-00044 at the Lobachevsky University of Nizhny Novgorod. RS has been also partially supported by CNPq, Conselho Nacional de Desenvolvimento Científico e Tecnológico - Brasil.

[†]amadeu.delshams@upc.edu

[‡]rodrigo.schaefer@upc.edu

Theorem 1. *Assume that $a_1 a_2 \neq 0$ and $k_1 l_2 - k_2 l_1 \neq 0$ in Hamiltonian (1)-(2). Then, for any $I^* > 0$, there exists $\varepsilon^* = \varepsilon^*(I^*, a_1, a_2) > 0$ such that for any ε , $0 < \varepsilon < \varepsilon^*$, there exists a trajectory $(p(t), q(t), I(t), \varphi(t))$ such that for some $T > 0$*

$$I(0) \leq -I^* < I^* \leq I(T).$$

Remark 2. For a rough estimate of $\varepsilon^* \sim \exp(-\pi I^*/2)$ at least for $|a_1/a_2| < 0.625$, $k_1 = l_2 = 1$ and $l_1 = k_2 = 0$, and of the diffusion time $T = T(\varepsilon^*, I^*, a_1, a_2) \sim (T_s(I^*, a_1, a_2)/\varepsilon) \log(C(I^*, a_1, a_2)/\varepsilon)$ the reader is referred to [DS17]. Analogous estimates could be obtained for all the other values of the parameters.

The proof is based on the geometrical method introduced in [DLS06] and relies on the concrete computation of several *scattering maps*. A scattering map is a map of transverse homoclinic orbits to a *normally hyperbolic invariant manifold* (NHIM). For Hamiltonian (1), the NHIM turns out to be simply

$$\tilde{\Lambda}_\varepsilon = \tilde{\Lambda} = \{(0, 0, I, \varphi, s) : (I, \varphi, s) \in \mathbb{R} \times \mathbb{T}^2\}. \quad (3)$$

In the unperturbed case, i.e., $\varepsilon = 0$, for any $I^* > 0$ the NHIM $\tilde{\Lambda}$ possesses a 4D *separatrix*, that is to say, coincident stable and unstable invariant manifolds

$$W^0 \tilde{\Lambda} = \{(p_0(\tau), q_0(\tau), I, \varphi, s) : \tau \in \mathbb{R}, I \in [-I^*, I^*], (\varphi, s) \in \mathbb{T}^2\},$$

where (p_0, q_0) are the separatrices to the saddle equilibrium point of the pendulum

$$(p_0(t), q_0(t)) = \left(\frac{\pm 2}{\cosh t}, 4 \arctan e^{\pm t} \right).$$

In the perturbed case, i.e., for small $\varepsilon > 0$, $W^u(\tilde{\Lambda}_\varepsilon)$ and $W^s(\tilde{\Lambda}_\varepsilon)$ do not coincide (this is the so-called splitting of separatrices), and every local transversal intersection between them gives rise to a (local) scattering map which is simply the correspondence between a past asymptotic motion in the NHIM to the corresponding future asymptotic motion following a homoclinic orbit. Since the NHIM has also an inner dynamics, an adequate combination of these two dynamics on the NHIM, the inner one and the outer one provided by the scattering map, generates the global instability (also called in short *Arnold diffusion*) as long as the outer dynamics does not preserve the invariant objects of the inner dynamics.

The inner motion is described in Section 2, the scattering maps in Section 3 and the absence of invariant sets in both dynamics is checked in Section 4, which also includes the proof of Theorem 1. Section 5 deals with the construction of a piecewise smooth global scattering map which is introduced as a possible new tool to design fast and simple paths of global instability. We finish this Introduction with some remarks about the necessity of the assumptions, as well as other features of the scattering map and a discussion of the model chosen and related work.

1.2 Necessity of the assumptions

If the determinant $\Delta := k_1 l_2 - k_2 l_1$ or some coefficient a_1, a_2 vanishes, for instance, if there is only one harmonic in g , there is no global instability for the action I . Indeed, looking at the equations associated to Hamiltonian (1)

$$\begin{aligned} \dot{q} &= \pm p & \dot{p} &= [\pm 1 + \varepsilon (a_1 \cos(k_1 \varphi + l_1 s) + a_2 \cos(k_2 \varphi + l_2 s))] \sin q \\ \dot{\varphi} &= I & \dot{I} &= \varepsilon \cos q (k_1 a_1 \sin(k_1 \varphi + l_1 s) + k_2 a_2 \sin(k_2 \varphi + l_2 s)) \\ \dot{s} &= 1 \end{aligned} \quad (4)$$

this is clear for $k_1 = k_2 = 0$, since in this case I is a constant of motion. If k_1 or $k_2 \neq 0$, say $k_1 \neq 0$, the change of variables

$$\bar{\varphi} = k_1 \varphi + l_1 s, \quad r\bar{\varphi} - \bar{s} = k_2 \varphi + l_2 s, \quad \bar{I} = k_1 I + l_1,$$

where $r = k_2/k_1$ can be assumed to satisfy $0 \leq r \leq 1$ without loss of generality, casts system (4) into

$$\begin{aligned}\dot{q} &= \pm p & \dot{p} &= [\pm 1 + \varepsilon (a_1 \cos \bar{\varphi} + a_2 \cos(r\bar{\varphi} - \bar{s}))] \sin q \\ \dot{\bar{\varphi}} &= \bar{I} & \dot{\bar{I}} &= \varepsilon k_1^2 \cos q (a_1 \sin \bar{\varphi} + r a_2 \sin(r\bar{\varphi} - \bar{s})) \\ \dot{\bar{s}} &= \Delta/k_1\end{aligned}$$

which is a Hamiltonian system with the Hamiltonian given by

$$\bar{H}_\varepsilon(p, q, \bar{I}, \bar{\varphi}, \bar{s}) = \pm \left(\frac{p^2}{2} + \cos q - 1 \right) + \frac{\bar{I}^2}{2} + \varepsilon k_1^2 \cos q (a_1 \cos \bar{\varphi} + a_2 \cos(r\bar{\varphi} - \bar{s})). \quad (5)$$

If $\Delta = 0$ Hamiltonian (5) is autonomous with 2 degrees of freedom, and therefore a global drift for the action I is not possible. Only drifts of size $\sqrt{\varepsilon}$ are possible due to KAM theorem. Analogously one easily checks that for $a_1 a_2 = 0$ Hamiltonian (1) is integrable or autonomous.

1.3 Reduction of the harmonic types

Under the hypothesis $(k_1 l_2 - k_2 l_1) a_1 a_2 \neq 0$ of Theorem 1, we first notice that the case $k_2 = 0$ of Theorem 1 is already proven in [DS17]. Indeed, $k_2 = 0$ implies $r := k_2/k_1 = 0$ and it turns out from (5) that Hamiltonian (1) is equivalent to the one with $k_1 = 1, k_2 = 0, l_1 = 0, l_2 = 1$:

$$H_\varepsilon(p, q, I, \varphi, t) = \pm \left(\frac{p^2}{2} + \cos q - 1 \right) + \frac{I^2}{2} + \varepsilon \cos q (a_1 \cos \varphi + a_2 \cos s), \quad (6)$$

which is just the Hamiltonian studied in [DS17]. Therefore, we only need to prove Theorem 1 for $k_1 k_2 \neq 0$ or equivalently for $r \in (0, 1]$. For the sake of clarity we will explain in full detail and prove Theorem 1 along Sections 2-4 just for $r = 1$, which by (5) is equivalent to the case $k_1 = 1, k_2 = 1, l_1 = 0, l_2 = -1$:

$$H_\varepsilon(p, q, I, \varphi, t) = \pm \left(\frac{p^2}{2} + \cos q - 1 \right) + \frac{I^2}{2} + \varepsilon \cos q (a_1 \cos \varphi + a_2 \cos(\varphi - s)). \quad (7)$$

To finish the proof of Theorem 1, in Section 4 we will sketch the modifications needed for the case $r \in (0, 1)$.

1.4 Scattering map types

By the definition given at the beginning of Section 3, a scattering map is in principle only *locally* defined, that is, for a small ball of values of the variables (I, φ, s) or $(I, \theta = \varphi - Is)$, since it depends on a non-degenerate critical point $\tau^* = \tau^*(I, \varphi, s)$ of a real function (16), depending smoothly on the variables (I, φ, s) , already introduced in [DLS06]. In the study carried out in Section 3, it will be described whether, in terms of the parameter $\mu := a_1/a_2$ and the variable I , a local scattering map can or cannot be smoothly defined for all the values of the angles (φ, s) or $\theta = \varphi - Is$, becoming thus a *global* or *extended* scattering map. This description will depend essentially on a geometrical characterization of the function $\tau^*(I, \varphi, s)$ in terms of the intersection of *crests* and *NHIM lines*, following [DH11]. Any degeneration of the critical point $\tau^* = \tau^*(I, \varphi, s)$ may give rise to more non-degenerate critical points and a bifurcation to *multiple* local scattering maps or to a non global scattering map. Different critical points $\tau^* = \tau^*(I, \varphi, s)$ give rise to different local scattering maps, and putting together different local scattering maps, one can sometimes obtain *piecewise smooth* global scattering maps, which are very useful to design paths of instability for the action I , and are simply called diffusion paths.

For instance, in the paper [DS17] devoted to the Hamiltonian (6), it was proven that for $0 < \mu = a_1/a_2 < 0.625$, there exist two different global scattering maps. Among the different kinds of associated orbits of these scattering maps, there appeared two of them called *highways*,

where the drift of the action I was very fast and simple. As will be described in Section 3, such highways do not appear for Hamiltonian (7). Nevertheless, as will be proven in Section 5, there exist piecewise smooth global scattering maps, and the possible diffusion along the discontinuity sets opens the possibility of applying the theory of piecewise smooth dynamical systems [Fil88].

1.5 About the model chosen and related work

Hamiltonian (1) is a standard example of an *a priori unstable* Hamiltonian system [CG94] formed by a pendulum, a rotor and a perturbation. It is usual in the literature to choose a perturbation depending periodically only on the positions—which turn out to be angles in our case—and time. Our perturbation $h(q, \varphi, s)$ (2) is a little bit special since it is a product of a function $f(q)$ times a function $g(\varphi, s)$. This choice makes easier the computations of the Poincaré-Melnikov potential (17), which is based on the Cauchy’s residue theorem. Theorem 1 can be easily generalized to any trigonometric polynomial or meromorphic function $f(q)$, although the computations of poles of high order become more complicated. In the same way, it could also be generalized to more general perturbations $h(q, \varphi, s)$, as long that h is a trigonometric polynomial or meromorphic in q . The dependence on more than two harmonics gives rise to the appearance of more resonances in the inner dynamics, which requires more control of their sizes, see for instance [DS97, DH09]. Apart from more difficulty in the computations of the Poincaré-Melnikov potential and the inner Hamiltonian, we do not foresee substantial changes, so we believe that Hamiltonian (1) could be considered as a paradigmatic example of an *a priori unstable* Hamiltonian system.

This paper is a natural culmination of [DS17], which dealt with the simpler Hamiltonian (6), and where a detailed description of NHIM lines and crests was carried out. An “optimal” estimate of the diffusion time close to some special orbits of the scattering map, called *highways*, was also given there. The study in this paper of Hamiltonian (7) is more complicated, due to a greater complexity of the evolution of the NHIM lines and crests with respect to the action I and the parameters of the system. In particular, the absence of highways prevents us of showing an estimate of diffusion time close to them.

The paper [DS17] also contains a fairly extensive list of references about global instability. Let us simply mention some new references that are not there, like [DT16] which contains a similar approach to the function τ^* of [DLS06] and the crests of [DH11], and the recent preprints [GT17, LMS16, Mar16, GM17, Che17] involving the geometrical method or variational methods.

We finish this introduction by noticing that in this paper we stress the interaction between NHIM lines and crests, since this allows us to describe the diverse scattering maps, as well as their domains, that appear in our problem. In more complicated models of Celestial Mechanics the Melnikov potential is not available. In these cases the computations of scattering maps rely on the numerical computation of invariant manifolds of a NHIM or some of its selected invariant objects, and the search of diffusion orbits is performed in a more crafted way (see [CDMR06, DMR08, DGR13, CGL16, DGR16]).

2 Inner dynamics

The inner dynamics is derived from the restriction of H_ε in (7) and its equations to $\tilde{\Lambda}$, that is,

$$K(I, \varphi, s) = \frac{I^2}{2} + \varepsilon (a_1 \cos \varphi + a_2 \cos(\varphi - s)), \quad (8)$$

and differential equations

$$\dot{\varphi} = I \quad \dot{s} = 1 \quad \dot{I} = \varepsilon (a_1 \sin \varphi + a_2 \sin(\varphi - s)). \quad (9)$$

Note that in this case the inner dynamics is slightly more complicated to describe than in [DS17] where there was just one resonance, namely, in $I = 0$. In the current case we have two

resonant regions of size $\mathcal{O}(\sqrt{\varepsilon})$ where secondary KAM tori appear. To describe these regions, we use normal forms as in [DLS06].

Consider the autonomous extended Hamiltonian

$$\bar{K}(I, A, \varphi, s) = \frac{I^2}{2} + A + \varepsilon(a_1 \cos \varphi + a_2 \cos(\varphi - s)), \quad (10)$$

with the differential equations

$$\begin{aligned} \dot{\varphi} &= I & \dot{I} &= \varepsilon(a_1 \sin \varphi + a_2 \sin(\varphi - s)) \\ \dot{s} &= 1 & \dot{A} &= -\varepsilon a_2 \sin(\varphi - s). \end{aligned}$$

This system is equivalent to the system represented by (8)+(9). We wish to eliminate the dependence on the angle variables. Consider a change of variables ε -close to the identity

$$(\varphi, s, I, A) = g(\phi, \sigma, J, B) = (\phi, \sigma, J, B) + \mathcal{O}(\varepsilon)$$

such that it is the one-time flow for a Hamiltonian εG , i.e., $g = g_{t=1}$, where g_t is solution of

$$\frac{dg_t}{dt} = J_0 \nabla \varepsilon G \circ g_t, \text{ where } J_0 \text{ is the symplectic matrix } \begin{pmatrix} 0 & 1 \\ -1 & 0 \end{pmatrix}.$$

Composing \bar{K} with g and expanding in a Taylor series around $t = 0$, one obtains

$$\bar{K} \circ g = \bar{K} + \{\bar{K}, \varepsilon G\} + \frac{1}{2} \{\{\bar{K}, \varepsilon G\}, \varepsilon G\} + \dots,$$

where $\{\cdot, \cdot\}$ is the Poisson bracket. Using the expansion (10) of \bar{K} , the equation above can be written as

$$\begin{aligned} \bar{K} \circ g &= \frac{J^2}{2} + B + \varepsilon \left(a_1 \cos \phi + a_2 \cos(\phi - \sigma) + \left\{ \frac{J^2}{2} + B, G \right\} \right) \\ &\quad + \frac{\varepsilon^2}{2} \left\{ \left\{ \frac{J^2}{2} + B, G \right\}, G \right\} + \mathcal{O}(\varepsilon^3). \end{aligned} \quad (11)$$

We want to find G such that $a_1 \cos \phi + a_2 \cos(\phi - \sigma) + \left\{ \frac{J^2}{2} + B, G \right\} = 0$, or equivalently,

$$J \frac{\partial G}{\partial \phi} + \frac{\partial G}{\partial \sigma} = a_1 \cos \phi + a_2 \cos(\phi - \sigma).$$

Given $a < b < 1$, consider any function $\Psi \in C^\infty(\mathbb{R})$ satisfying $\Psi(x) = 1$ for $x \in [-a, a]$ and $\Psi(x) = 0$ for $|x| > b$ and introduce

$$G(J, B, \phi, \sigma) := \frac{a_1}{J} (1 - \Psi(J)) \sin \phi + \frac{a_2}{J-1} (1 - \Psi(J-1)) \sin(\phi - \sigma),$$

Substituting the above function $G(J, B, \phi, \sigma)$ in (11) we have

$$\bar{K} \circ g = \frac{J^2}{2} + B + \mathcal{O}(\varepsilon^2), \quad (12)$$

for $J, J-1 \notin [-b, b]$. For $J \in [-a, a]$,

$$\bar{K} \circ g = \frac{J^2}{2} + B + \varepsilon a_1 \cos \phi + \mathcal{O}(\varepsilon^2). \quad (13)$$

Finally, for $J-1 \in [-a, a]$,

$$\bar{K} \circ g = \frac{J^2}{2} + B + \varepsilon a_2 \cos(\phi - \sigma) + \mathcal{O}(\varepsilon^2). \quad (14)$$

From (13) and (14), one sees that on $J = 0$ and $J = 1$ there are resonances of first order in ε with a pendulum-like behavior.

Coming back to the original variables, three kinds of invariant tori are obtained. For the first order resonance $I = 0$, there is a positive \bar{a} such that the invariant tori are given by $F^0(I, \varphi, s) = \text{constant}$ with

$$F^0(I, \varphi, s) = \frac{I^2}{2} + \varepsilon a_1 \cos \varphi + \mathcal{O}(\varepsilon^2). \quad (15)$$

for $I \in [-\bar{a}, \bar{a}]$

Analogously, for the first order resonance $I = 1$, with

$$F^1(I, \varphi, s) = \frac{(I-1)^2}{2} + \varepsilon a_2 \cos(\varphi - s) + \mathcal{O}(\varepsilon^2),$$

for $I - 1 \in [-\bar{a}, \bar{a}]$.

Remark 3. As commented in [DLS06], there exists a *secondary* resonance in $I = 1/2$, but the size of the gap in its resonant region is much smaller than the size of gaps in resonant regions associated to $I = 0$ and $I = 1$.

Remark 4. In a more general case with $r \neq 1$, the resonances take place in $I = 0$ and $I = 1/r$.

From (12), on the non-resonant region the invariant tori has equations $F^{\text{nr}}(I) = \text{constant}$ with

$$F^{\text{nr}}(I) = \frac{I^2}{2} + \mathcal{O}(\varepsilon^2).$$

An illustration of the inner dynamics is displayed in Figure 1.

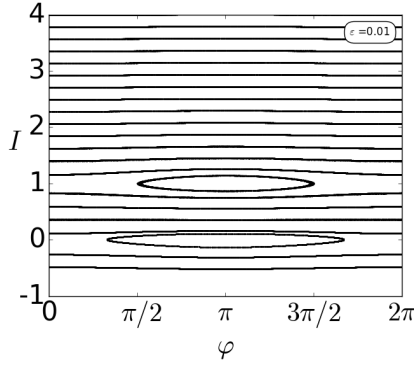


Fig. 1: Plane $\varphi \times I$ of inner dynamics for $\mu = 0.75$ and $\varepsilon = 0.01$.

3 Scattering map

3.1 Definition of scattering map

We are going to explore the properties of the scattering maps of Hamiltonian (7). The notion of scattering map on a NHIM was introduced in [DLS00]. Let W be an open set of $[-I^*, I^*] \times \mathbb{T}^2$ such that the invariant manifolds of the NHIM $\tilde{\Lambda}$ introduced in (3) intersect transversally along a homoclinic manifold $\Gamma = \{\tilde{z}(I, \varphi, s; \varepsilon), (I, \varphi, s) \in W\}$ so that for any $\tilde{z} \in \Gamma$ there exist unique $\tilde{x}_{+,-} = \tilde{x}_{+,-}(I, \varphi, s; \varepsilon) \in \tilde{\Lambda}$ such that $\tilde{z} \in W_\varepsilon^s(x_-) \cap W_\varepsilon^u(\tilde{x}_+)$. Let

$$H_{+,-} = \bigcup \{\tilde{x}_{+,-}(I, \varphi, s; \varepsilon) : (I, \varphi, s) \in W\}.$$

The scattering map associated to Γ is the map

$$\begin{aligned} S : H_- &\longrightarrow H_+ \\ \tilde{x}_- &\longmapsto S(\tilde{x}_-) = \tilde{x}_+. \end{aligned}$$

For the characterization of the scattering maps, it is required to select the homoclinic manifold Γ and this is done using the Poincaré-Melnikov theory. From [DLS06, DH11], we have the following proposition

Proposition 5. *Given $(I, \varphi, s) \in [-I^*, I^*] \times \mathbb{T}^2$, assume that the real function*

$$\tau \in \mathbb{R} \longmapsto \mathcal{L}(I, \varphi - I\tau, s - \tau) \in \mathbb{R} \quad (16)$$

has a non degenerate critical point $\tau^ = \tau^*(I, \varphi, s)$, where*

$$\mathcal{L}(I, \varphi, s) := \int_{-\infty}^{+\infty} (f(q_0(\sigma)) - f(0)) g(\varphi + I\sigma, s + \sigma; 0) d\sigma.$$

Then, for $0 < \varepsilon$ small enough, there exists a unique transversal homoclinic point \tilde{z} to $\tilde{\Lambda}_\varepsilon$ of Hamiltonian (1), which is ε -close to the point $\tilde{z}^(I, \varphi, s) = (p_0(\tau^*), q_0(\tau^*), I, \varphi, s) \in W^0(\tilde{\Lambda})$:*

$$\tilde{z} = \tilde{z}(I, \varphi, s) = (p_0(\tau^*) + O(\varepsilon), q_0(\tau^*) + O(\varepsilon), I, \varphi, s) \in W^u(\tilde{\Lambda}_\varepsilon) \cap W^s(\tilde{\Lambda}_\varepsilon).$$

The function \mathcal{L} is called the *Melnikov potential* of Hamiltonian (1). For the concrete Hamiltonian (7) it takes the form

$$\mathcal{L}(I, \varphi, s) = A_1(I) \cos \varphi + A_2(I) \cos(\varphi - s), \quad (17)$$

where

$$A_1(I) = \frac{2\pi I a_1}{\sinh(\pi I/2)} \quad \text{and} \quad A_2(I) = \frac{2\pi(I-1)a_2}{\sinh(\pi(I-1)/2)}.$$

The homoclinic manifold Γ is characterized by the function $\tau^*(I, \varphi, s)$. Once a $\tau^*(I, \varphi, s)$ is chosen, which under the conditions of Proposition 5, is locally smoothly well defined, by the geometric properties of the scattering map, see [DLS08, DH09, DH11], the scattering map has the explicit local form

$$S(I, \varphi, s) = \left(I + \varepsilon \frac{\partial L^*}{\partial \varphi}(I, \varphi, s) + \mathcal{O}(\varepsilon^2), \varphi - \varepsilon \frac{\partial L^*}{\partial I}(I, \varphi, s) + \mathcal{O}(\varepsilon^2), s \right),$$

where

$$L^*(I, \varphi, s) = \mathcal{L}(I, \varphi - I\tau^*(I, \varphi, s), s - \tau^*(I, \varphi, s)). \quad (18)$$

Notice that the variable s is fixed under the scattering map. As a consequence [DH11, DS17], introducing the variable

$$\theta = \varphi - Is$$

and defining the *reduced Poincaré function*

$$\mathcal{L}^*(I, \theta) := L^*(I, \varphi - Is, 0) = L^*(I, \varphi, s), \quad (19)$$

in the variables (I, θ) , the scattering map has the simple form

$$S(I, \theta) = \left(I + \varepsilon \frac{\partial \mathcal{L}^*}{\partial \theta}(I, \theta) + \mathcal{O}(\varepsilon^2), \theta - \varepsilon \frac{\partial \mathcal{L}^*}{\partial I}(I, \theta) + \mathcal{O}(\varepsilon^2) \right),$$

so up to $\mathcal{O}(\varepsilon^2)$ terms, $S(I, \theta)$ is the ε times flow of the *autonomous* Hamiltonian $-\mathcal{L}^*(I, \theta)$. In particular, the iterates under the scattering map follow the level curves of \mathcal{L}^* up to $\mathcal{O}(\varepsilon^2)$.

3.2 Crests and NHIM lines

We have seen that the function τ^* plays a central role in our study. Therefore, we are interested in finding the critical points $\tau^* = \tau^*(I, \varphi, s)$ of function (16). For our concrete case (17), τ^* is a solution of

$$IA_1(I) \sin(\varphi - I\tau^*) + (I - 1)A_2(I) \sin(\varphi - s - (I - 1)\tau^*) = 0. \quad (20)$$

This equation can be viewed from two equivalently geometrical viewpoints. The first one is that to find $\tau^* = \tau^*(I, \varphi, s)$ satisfying (20) for any $(I, \varphi, s) \in [-I^*, I^*] \times \mathbb{T}^2$ is the same as to look for the extrema of \mathcal{L} on the *NHIM line*

$$R(I, \varphi, s) = \{(I, \varphi - I\tau, s - \tau) : \tau \in \mathbb{R}\}. \quad (21)$$

Remark 6. Since $(\varphi, s) \in \mathbb{T}^2$, $R(I, \varphi, s)$ is a closed line if $I \in \mathbb{Q}$ and it is a dense line on $\{I\} \times \mathbb{T}^2$ if $I \notin \mathbb{Q}$.

The other viewpoint is that, fixing (I, φ, s) , a solution τ^* of (20) is equivalent to finding intersections between a NHIM line (21) and a curve defined by

$$IA_1(I) \sin \varphi + (I - 1)A_2(I) \sin(\varphi - s) = 0. \quad (22)$$

These curves are called *crests*, and in a general way can be defined as follows.

Definition 7. [DH11] We define by *Crests* $\mathcal{C}(I)$ the curves on (I, φ, s) , $(\varphi, s) \in \mathbb{T}^2$, such that

$$\frac{\partial \mathcal{L}}{\partial \tau}(I, \varphi - I\tau, s - \tau)|_{\tau=0} = 0, \quad (23)$$

or equivalently,

$$I \frac{\partial \mathcal{L}}{\partial \varphi}(I, \varphi, s) + \frac{\partial \mathcal{L}}{\partial s}(I, \varphi, s) = 0.$$

As in our case $\mathcal{L}(I, \varphi - I\tau, s - \tau) = A_1(I) \cos(\varphi - I\tau) + A_2(I) \cos(\varphi - s - (I - 1)\tau)$, equation (23) takes the form (22). Introducing

$$\sigma = \varphi - s, \quad (24)$$

equation (22) can be rewritten as

$$\mu \alpha(I) \sin \varphi + \sin \sigma = 0, \quad (25)$$

for $I \neq 1$, where

$$\mu = \frac{a_1}{a_2} \quad \text{and} \quad \alpha(I) = \frac{I^2 \sinh(\frac{\pi}{2}(I - 1))}{(I - 1)^2 \sinh(\frac{\pi I}{2})}. \quad (26)$$

From now on, when we refer to crests $\mathcal{C}(I)$ we mean the set of points (I, φ, σ) satisfying equation (25). See an illustration in Fig. 3.

Remark 8. In [DS17] the crests were described on the plane (φ, s) , whereas now such curves lie on the plane (φ, σ) . Besides, differently from the cases studied in [DH11, DS17], the function $\alpha(I)$ is not defined for all I . More precisely, it is not defined for $I = 1$. For this value of I , equation (25) is not adequate, and one has to use (22) to check that for $I = 1$ the crests are just two vertical straight lines on the plane (φ, σ) given by $\varphi = 0$ and $\varphi = \pi$.

Remark 9. For Hamiltonian (5) and $r \in (0, 1)$, $\alpha_r(I)$ is not defined for $I = 1/r$ and is given by

$$\alpha_r(I) = \frac{I^2 \sinh(\frac{\pi}{2}(rI - 1))}{(rI - 1)^2 \sinh(\frac{\pi I}{2})}.$$

We are interested in understanding the behavior of these crests because, as we have seen in previous works [DH11, DS17], their intersection with the NHIM lines determine the existence and behavior of scattering maps.

From (25), when $|\alpha(I)| < 1/|\mu|$, σ can be written as a function of φ for all $\varphi \in \mathbb{T}$ on the crest $\mathcal{C}(I)$. On the other hand, if $|\alpha(I)| > 1/|\mu|$, φ can be written as a function of σ for all $\sigma \in \mathbb{T}$. These two conditions give us two kinds of crests: *horizontal* for $|\alpha(I)| < 1/|\mu|$ and *vertical* for $|\alpha(I)| > 1/|\mu|$. These names are due to their forms on the plane (φ, σ) . We consider the same characterization used in [DS17]:

- For $|\alpha(I)| < 1/|\mu|$, there are two horizontal crests $\sigma = \xi_{M,m}(I, \varphi)$

$$\mathcal{C}_{M,m}(I) = \{(I, \varphi, \xi_{M,m}(I, \varphi)) : \varphi \in \mathbb{T}\},$$

$$\begin{aligned} \xi_M(I, \varphi) &= -\arcsin(\mu\alpha(I) \sin \varphi) \quad \text{mod } 2\pi \\ \xi_m(I, \varphi) &= \arcsin(\mu\alpha(I) \sin \varphi) + \pi \quad \text{mod } 2\pi. \end{aligned} \quad (27)$$

- For $|\alpha(I)| > 1/|\mu|$, there are two vertical crests $\varphi = \eta_{M,m}(I, \sigma)$

$$\mathcal{C}_{M,m}(I) = \{(I, \eta_{M,m}(I, \sigma), \sigma) : \sigma \in \mathbb{T}\},$$

$$\begin{aligned} \eta_M(I, \sigma) &= -\arcsin(\sin \sigma / (\mu\alpha(I))) \quad \text{mod } 2\pi \\ \eta_m(I, \sigma) &= \arcsin(\sin \sigma / (\mu\alpha(I))) + \pi \quad \text{mod } 2\pi. \end{aligned}$$

Remark 10. $|\alpha(I)| = 1/|\mu|$ is a singular or bifurcation case. In this case, the crests are straight lines and are not differentiable in $\varphi = \pi/2$ and $\varphi = 3\pi/2$. See Fig. 6 of [DS17].

Remark 11. The crest containing the point $(\varphi, \sigma) = (0, 0)$ will be denoted by $\mathcal{C}_M(I)$ and the crest containing the point $(\varphi, \sigma) = (\pi, \pi)$ by $\mathcal{C}_m(I)$.

Note that the function $|\alpha(I)|$ is not bounded, indeed

$$\lim_{I \rightarrow 1} |\alpha(I)| = +\infty.$$

This implies that for any μ there exists a neighborhood U of $I = 1$ such that for all $I \in U$ the crests are vertical. On the other hand, since $\alpha(0) = 0$ there exists a neighborhood V of $I = 0$ such that for all $I \in V$ the crests are horizontal. We notice here a remarkable difference with the Hamiltonians studied in [DH11, DS17], where, for $|\mu| \leq 0.97$, all the crests are horizontal for all I .

Now take a look at the properties of the function $\alpha(I)$ introduced in (26) to describe under which conditions in μ the crests are horizontal or vertical. First of all, observe that for $I \neq 1$, $\alpha(I)$ is smooth and $\alpha'(I) \neq 0$, and for $I = 1$ $\alpha(I)$ is not bounded, indeed it has a vertical asymptote

$$\lim_{I \rightarrow 1^-} \alpha(I) = -\infty \quad \text{and} \quad \lim_{I \rightarrow 1^+} \alpha(I) = +\infty.$$

Given a $\mu \neq 0$, since $\alpha(0) = 0$, there exists a unique $I_c \in (0, 1)$ such that $|\alpha(I)| = 1/|\mu|$. So, the crests are horizontal for $I \in [0, I_c)$ and vertical for $I \in (I_c, 1)$.

Others important limits are

$$\lim_{I \rightarrow -\infty} \alpha(I) = \exp(\pi/2) \quad \text{and} \quad \lim_{I \rightarrow +\infty} \alpha(I) = \exp(-\pi/2).$$

The first limit implies that $|\alpha(I)| < \exp(\pi/2)$ for $I \in (-\infty, 0)$. Thus, if $\exp(\pi/2) \leq 1/|\mu|$ the crests are horizontal for $I \in (-\infty, 0)$. Otherwise, if $1/|\mu| < \exp(\pi/2)$, there exists a unique $I_1 \in (-\infty, 0)$ such that $|\alpha(I)| = 1/|\mu|$ and the crests are vertical for $I \in (-\infty, I_1)$ and horizontal for $I \in (I_1, 0)$.

The second limit implies that $|\alpha(I)| > \exp(-\pi/2)$ for $I \in (1, +\infty)$. Then, if $\exp(-\pi/2) \geq 1/|\mu|$, the crests are vertical for $I \in [1, +\infty)$. if $\exp(-\pi/2) < 1/|\mu|$, there exists a unique $I_r \in (1, +\infty)$, such that the crests are vertical for any I in $[1, I_r)$ and horizontal for $I \in (I_r, +\infty)$.

Summarizing, for $1/|\mu| \geq \exp(\pi/2)$, crests are horizontal for $I \in (-\infty, I_c) \cup (I_r, +\infty)$ and vertical for $I \in (I_c, I_r)$. For $\exp(-\pi/2) < 1/|\mu| < \exp(\pi/2)$, crests are horizontal for $I \in (I_1, I_c) \cup (I_r, +\infty)$ and vertical for $I \in (-\infty, I_1) \cup (I_c, I_r)$. Finally, if $1/|\mu| < \exp(-\pi/2)$, crests are horizontal for $I \in (I_1, I_c)$ and vertical for $I \in (-\infty, I_1) \cup (I_c, +\infty)$.

Remark 12. For $r \in (0, 1)$, $\alpha_r(I)$ is not bounded on a neighbourhood of the resonance $I = 1/r$, i.e., $\lim_{I \rightarrow 1/r^-} \alpha_r(I) = -\infty$ and $\lim_{I \rightarrow 1/r^+} \alpha_r(I) = +\infty$. The same behavior takes place for $r = 1$ and close to $I = 1$. On the other hand, for $I \rightarrow \pm\infty$, $\alpha_r(I)$ has the same behavior as in the case for $r = 0$, $\lim_{I \rightarrow \pm\infty} \alpha_r(I) = 0$. This implies that for any value of μ , for I close enough to $I = 1/r$ the crests are vertical, and for $|I|$ large enough the crests are horizontal.

Example To illustrate this discussion, we present a concrete example. Taking $\mu = 0.5$, we have $\exp(-\pi/2) < 1/\mu = 2 < \exp(\pi/2)$. In this case we have $I_1 \approx -1.807$, $I_c \approx 0.701$ and $I_r \approx 1.367$. The crests are horizontal in $(-1.807, 0.701) \cup (1, 367, +\infty)$ and vertical in $(-\infty, -1.807) \cup (0.701, 1.367)$. We emphasize that this scenario is very different from the case in [DS17]. There, for $\mu = 0.5$ the crests are horizontal for all I .

Now, we are going to focus on the transversality of the intersection between NHIM lines $R(I, \varphi, s)$ and crests $\mathcal{C}(I)$. On the plane (φ, σ) the NHIM lines can be written as

$$R_I(\varphi, \sigma) = \{(\varphi - I\tau, \sigma - (I - 1)\tau), \tau \in \mathbb{R}\}, \quad (28)$$

so that its slope is $(I - 1)/I$ in such plane. Therefore, there exists an intersection between NHIM lines and crests that is not transversal if, and only if, there exists a tangent vector of $\mathcal{C}(I)$ at a point that is parallel to $(I, I - 1)$, or, using the parameterizations,

$$\frac{\partial \xi}{\partial \varphi}(I, \varphi) = \frac{I - 1}{I} \quad \text{or} \quad \frac{\partial \eta}{\partial \sigma}(I, \sigma) = \frac{I}{I - 1}.$$

Considering a *horizontal* parameterization of $\mathcal{C}(I)$, the tangency condition is equivalent to

$$\frac{\pm \alpha(I) \mu \cos \varphi}{\sqrt{1 - \mu^2 \alpha^2(I) \sin^2 \varphi}} = \frac{I - 1}{I}.$$

Therefore, there exists a φ satisfying the above condition if, and only if,

$$|\beta(I)| \geq \frac{1}{|\mu|}, \quad \text{where} \quad \beta(I) = \frac{I \alpha(I)}{I - 1}$$

and φ takes the form

$$\varphi = \pm \arctan \left(\sqrt{\frac{\beta(I)^2 - (1/\mu)^2}{(1/\mu)^2 - \alpha(I)^2}} \right).$$

In an analogous way, for a *vertical* parameterization $\eta(I, \sigma)$, there are tangencies if, and only if,

$$|\beta(I)| \leq \frac{1}{|\mu|} \quad \text{with} \quad \sigma = \pm \arctan \left(\left| \frac{I - 1}{I} \right| \sqrt{\frac{(1/\mu)^2 - \beta(I)^2}{\alpha(I)^2 - (1/\mu)^2}} \right).$$

Remark 13. Observe that in both cases, horizontal and vertical crests, there are tangencies if, and only if,

$$\left(|\alpha(I)| - \frac{1}{|\mu|} \right) \left(|\beta(I)| - \frac{1}{|\mu|} \right) < 0.$$

The function $|\beta(I)|$ is smooth in $\mathbb{R} \setminus \{1\}$ and $d|\beta(I)|/dI = 0$ only for $I = 0$. Besides, we have

$$\lim_{I \rightarrow 1} |\beta(I)| = +\infty, \quad \lim_{I \rightarrow -\infty} |\beta(I)| = \exp(\pi/2) \quad \text{and} \quad \lim_{I \rightarrow +\infty} |\beta(I)| = \exp(-\pi/2).$$

Therefore, there are three possibilities:

- for $1/|\mu| \geq \exp(\pi/2)$, there exist $I_0 \in (1/2, 1)$ and $I_+ \in (1, +\infty)$ such that I_0 and I_+ are solutions of $|\beta(I)| - 1/|\mu| = 0$. Besides, $|\beta(I)| < 1/|\mu|$ for $I \in (-\infty, I_0) \cup (I_+, +\infty)$ and $|\beta(I)| > 1/|\mu|$ for $I \in (I_0, 1) \cup (1, I_+)$.
- for $\exp(-\pi/2) < 1/|\mu| < \exp(\pi/2)$, there exist $I_- \in (-\infty, 0)$, $I_0 \in (0, 1)$ and $I_+ \in (1, +\infty)$ such that I_- , I_0 and I_+ are solutions of $|\beta(I)| - 1/|\mu| = 0$. Besides, $|\beta(I)| < 1/|\mu|$ for $I \in (I_-, I_0) \cup (I_+, +\infty)$ and $|\beta(I)| > 1/|\mu|$ for $I \in (-\infty, I_-) \cup (I_0, 1) \cup (1, I_+)$.
- For $1/|\mu| \leq \exp(-\pi/2)$, there exist $I_- \in (-\infty, 0)$ and $I_0 \in (0, 1/2)$ such that I_- and I_0 are solutions of $|\beta(I)| - 1/|\mu| = 0$. Besides, $|\beta(I)| < 1/|\mu|$ for $I \in (I_-, I_0)$ and $|\beta(I)| > 1/|\mu|$ for $I \in (-\infty, I_-) \cup (I_0, 1) \cup (1, \infty)$.

Putting together this description of $|\beta(I)|$ with the study about vertical and horizontal crests and adding that

$$\begin{aligned} |\beta(I)| &< |\alpha(I)| & \forall I \in (-\infty, 0) \cup (0, 1/2); \\ |\beta(I)| &> |\alpha(I)| & \forall I \in (1/2, 1) \cup (1, +\infty); \\ |\beta(0)| &= |\alpha(0)| = 0 & \quad |\beta(1/2)| = |\alpha(1/2)| = 1 \end{aligned}$$

we can state the proposition below.

Proposition 14. *Consider the two crests $\mathcal{C}(I)$ defined by (25) and the NHIM line $R_I(\varphi, \sigma)$ defined in (21) for Hamiltonian (7).*

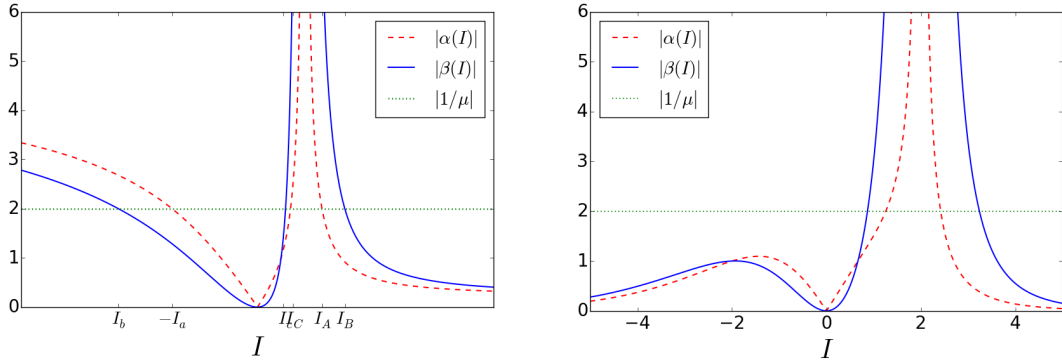
- For $|\mu| \leq \exp(-\pi/2)$, there exist $I_b < I_a < I_A < I_B$ such that
 - for $I < I_b$ or $I_B < I$, $\mathcal{C}(I)$ are horizontal and intersect transversally any $R_I(\varphi, \sigma)$;
 - for $I_b \leq I < I_a$ or $I_A < I \leq I_B$, the crests $\mathcal{C}(I)$ are horizontal, but now, there exist tangencies between $\mathcal{C}(I)$ and two NHIM lines $R_I(\varphi, \sigma)$;
 - for $I_a < I < I_A$, the crests $\mathcal{C}(I)$ are vertical and intersect transversally any $R_I(\varphi, \sigma)$.
- For $\exp(-\pi/2) < |\mu| < \exp(\pi/2)$ there exist $I_b < I_a < I_c \leq I_C < I_A < I_B$ such that
 - for $I < I_b$ or $I_C < I < I_A$, $\mathcal{C}(I)$ are vertical and intersect transversally any $R_I(\varphi, \sigma)$;
 - for $I_b \leq I < I_a$, the crests $\mathcal{C}(I)$ are vertical and there exist tangencies between $\mathcal{C}(I)$ and two NHIM lines $R_I(\varphi, \sigma)$;
 - for $I_a < I < I_c$ or $I_B < I$, $\mathcal{C}(I)$ are horizontal and intersect transversally any $R_I(\varphi, \sigma)$;
 - for $I_A \leq I \leq I_B$, the crests $\mathcal{C}(I)$ are horizontal and there exist tangencies between $\mathcal{C}(I)$ and two NHIM lines $R_I(\varphi, \sigma)$;
 - for $I_c \leq I \leq I_C$, if $I_c < 1/2$, the crests $\mathcal{C}(I)$ are vertical and there exist tangencies between $\mathcal{C}(I)$ and $R_I(\varphi, \sigma)$. If $I_c = 1/2$, from the properties of $\alpha(I)$ and $\beta(I)$ this interval is just one point. If $I_c > 1/2$, the crests $\mathcal{C}(I)$ are horizontal and there exist tangencies.
- For $|\mu| \geq \exp(\pi/2)$ there exist $I_b < I_a < I_A < I_B$ such that
 - for $I < I_b$ or $I_B < I$, $\mathcal{C}(I)$ are vertical and intersect transversally any $R_I(\varphi, \sigma)$;
 - for $I_b \leq I < I_a$ or $I_A < I \leq I_B$, the crests $\mathcal{C}(I)$ are vertical and there exist tangencies between $\mathcal{C}(I)$ and two NHIM lines $R_I(\varphi, \sigma)$;
 - for $I_a < I < I_A$, the crests $\mathcal{C}(I)$ are horizontal and intersect transversally any $R_I(\varphi, \sigma)$.

Remark 15. Note that we are not considering the singular case $|\alpha(I)| = 1/|\mu|$ described in Remark 10.

Example Again, to illustrate this proposition, we take the case with $\mu = 0.5$, see Fig. 2(a). In this case, we have $|\beta(I)| = 1/|\mu|$ for $I \approx -2.942, 0.595, 1.85$ and

- for $I \in (-\infty, -2.942) \cup (0.701, 1) \cup (1, 1.367) \Rightarrow \begin{cases} |\alpha(I)| > 1/|\mu| \Rightarrow \text{vertical crests} \\ |\beta(I)| > 1/|\mu| \Rightarrow \text{no tangencies} \end{cases}$
- for $I \in [-2.942, -1.807) \Rightarrow \begin{cases} |\alpha(I)| > 1/|\mu| \Rightarrow \text{vertical crests} \\ |\beta(I)| \leq 1/|\mu| \Rightarrow \text{tangencies} \end{cases}$
- for $I \in (-1.807, 0.595) \cup (1.85, +\infty) \Rightarrow \begin{cases} |\alpha(I)| < 1/|\mu| \Rightarrow \text{horizontal crests} \\ |\beta(I)| < 1/|\mu| \Rightarrow \text{no tangencies} \end{cases}$
- for $I \in [0.595, 0.701) \cup (1.367, 1.85] \Rightarrow \begin{cases} |\alpha(I)| < 1/|\mu| \Rightarrow \text{horizontal crests} \\ |\beta(I)| \geq 1/|\mu| \Rightarrow \text{tangencies} \end{cases}$

Once more, we compare with the Hamiltonian (6) studied in [DS17]. For Hamiltonian (6) and $\mu = 0.5$ there is no tangency, but for Hamiltonian (7) we can find tangencies for horizontal and vertical crests. Indeed, for Hamiltonian (6) and any $0 < |\mu| < 0.625$ there is no tangency, whereas for any $\mu \neq 0$ there are tangencies for Hamiltonian (7).



(a) $|\alpha(I)|$ and $|\beta(I)|$: $\mu = 0.5$, $I_b \approx -2.942$, $I_a \approx -1.807$, $I_c \approx 0.595$, $I_C \approx 0.701$, $I_A \approx 1.367$ and $I_B \approx 1.85$

(b) $|\alpha_r(I)|$ and $|\beta_r(I)|$: $\mu = 0.5$ and $r = 0.5$.

Fig. 2: $|\alpha(I)|$ and $|\beta(I)|$: Behavior of the crests and tangencies.

Remark 16. For $r \in (0, 1)$, $\beta_r(I)$ is defined by $\beta_r(I) = I\alpha_r(I)/(rI-1)$. In this case, $\lim_{I \rightarrow 1/r} |\beta_r(I)| = +\infty$ and $\lim_{I \rightarrow \pm\infty} |\beta_r(I)| = 0$. In Fig. 2(b), a comparison between the functions $\alpha_r(I)$, $\beta_r(I)$ and the straight line $1/|\mu|$ for $r = 1/2$ is displayed.

For each crest, where it is well defined, there exists, at least, a value τ^* such that

$$(\varphi - I\tau^*, \sigma - (I-1)\tau^*) = (\varphi - I\tau^*, \xi(I, \varphi - I\tau^*)) \text{ or } (\eta(I, \sigma - (I-1)\tau^*), \sigma - (I-1)\tau^*),$$

which means that $R_I(\varphi, \sigma) \cap \mathcal{C}(I) \neq \emptyset$. This intersection is intrinsically associated to a homoclinic orbit to the NHIM. To make a choice about how to take such τ^* is to choose in which homoclinic manifold Γ the homoclinic points \tilde{z}^* lie. Even more, it is to choose what scattering map we are going to use.

3.3 Construction of scattering maps

We have now several goals. First, to explain, given (I, θ) , how to find the intersection between one of the NHIM lines and one of the two crests, and consequently, to define the function τ^* .

(27). In the same way, we can separate completely the scattering maps associated to the horizontal crests and the scattering maps associated to the vertical crests. Notice that the scattering maps associated to horizontal crests are defined only for values of I satisfying $|\alpha(I)| < 1/|\mu|$ whereas the scattering maps associated to the vertical crests are defined only for values of I satisfying $|\alpha(I)| > 1/|\mu|$.

As noted previously, crests are vertical in a neighborhood of $I = 1$ for any value of μ . Therefore, there is no scattering map associated to a horizontal crest close to $I = 1$. Analogously, since $|\alpha(0)| = 0$, crests are horizontal in a neighborhood of $I = 0$ for any value of μ and, therefore, there is no scattering map associated to a vertical crest close to $I = 0$. This implies that these “horizontal” or “vertical” scattering maps are just locally defined, in other words, they are not defined on the whole plane (θ, I) . This motivates to define *global scattering maps*. Global scattering maps are important because they describe the outer dynamics for large intervals of I and are defined as follows

Definition 17. A scattering map $\mathcal{S}(I, \theta)$ is called a *global scattering map* if it is defined on all $\theta \in \mathbb{T}$ for any fixed I .

Note that $\mathcal{S}(I, \theta)$ is a global scattering map as long as $\tau^*(I, \theta)$ is a global function, i.e., defined on all $\theta \in \mathbb{T}$ for any fixed I . If $\tau^*(I, \theta)$ is smoothly defined, the same will happen to $\mathcal{S}(I, \theta)$. Tangencies between NHIM lines and crests, as well as discontinuities in their intersections give rise to non-smooth scattering maps.

Remark 18. For instance, in the paper [DS17] devoted to the Hamiltonian (6), it was proven that for $0 < \mu = a_1/a_2 < 0.625$, there exist two different global scattering maps. Let us add that for $0.625 \leq \mu < 0.97$, due to the existence of tangencies between the NHIM lines and the crests, there appear two or six scattering maps. Such *multiple* scattering maps are indeed piecewise smooth global scattering maps, see Figs. 9–11 of [DS17]. Their discontinuities lie along the *tangency locus* and were avoided there to construct diffusion paths, just for the sake of simplicity.

For Hamiltonian (7), to extend scattering maps which are in principle only locally defined we have now two options: to combine a scattering map associated to a horizontal crest with a scattering map associated to a vertical crest or to extend the previously called “horizontal” or “vertical” scattering maps. Although the first option may provide a global scattering map, they may appear complex discontinuity sets which give rise to a complicated phase space.

The second option is to apply the same idea used in [DS17] when we defined the scattering map “with holes”. When $|\alpha(I)| > 1/|\mu|$, the horizontal crests are no longer defined for all $\varphi \in \mathbb{T}$, indeed, they become vertical crests defined for all $\sigma \in \mathbb{T}$. Nevertheless, the vertical crests are formed by pieces of horizontal crests. This implies that even for these values of I we can use ξ given in (27) to parameterize some intersections between $R(I, \varphi, \sigma)$ and $\mathcal{C}(I)$. As we can see in Fig. 4, the vertical and horizontal crest \mathcal{C}_M are very close in a neighbourhood of $\varphi = 0$. When we have a bifurcation from horizontal to vertical crests (or vice versa), it is natural just to change the parameterization from ξ_M to η_M for these values of φ . With this choice the orbits of the scattering map are continuous for θ close to 0 or 2π . The same happens with ξ_m and η_m for values of φ close to π . Scattering maps associated to horizontal crests for values of I satisfying $|\mu\alpha(I)| < 1$ are defined for all $\varphi \in \mathbb{T}$. The extension of them to values of I for $\varphi \in \mathbb{T}$ such that $|\mu\alpha(I) \sin \varphi| < 1$ are called *extended scattering maps*.

Definition 19. A scattering map $\mathcal{S}(I, \theta)$ is called an *extended scattering map* if it is associated to horizontal crests for which $|\mu\alpha(I)| < 1$, and is continuously extended to the pieces of the vertical crests where they behave as horizontal crests, that is, for the values φ such that $|\mu\alpha(I) \sin \varphi| < 1$.

Since we have already seen in Proposition 14 that there exist tangencies between NHIM lines and crests for any value of μ , there are no global scattering maps for Hamiltonian (7). However, there exist extended scattering maps with a domain large enough to provide diffusion paths.

To illustrate the current scenario we will display the level curves of the reduced Poincaré function $\mathcal{L}^*(I, \theta)$ defined in (19), which up to $\mathcal{O}(\varepsilon^2)$ contain orbits of the scattering map $\mathcal{S}(I, \theta)$.

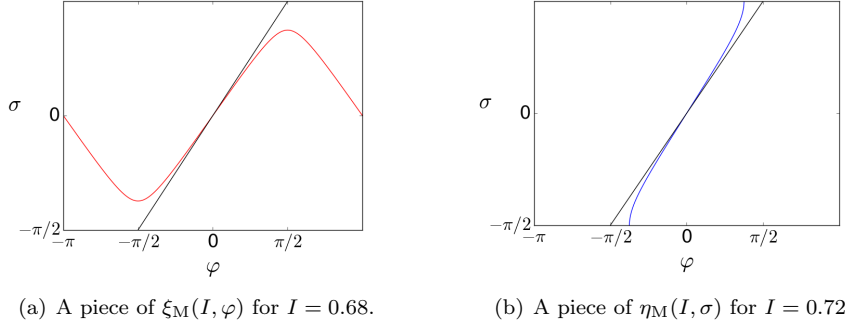


Fig. 4: Comparison between $\xi_M(I, \varphi)$ and $\eta_M(I, \sigma)$ for $\mu = 0.5$, $I = 0.68$ and $I = 0.72$ respectively.

We begin by considering $\mu = 0.6$ and the horizontal crest $\mathcal{C}_M(I)$. In Fig. 5(a) we display the scattering map built using τ^* defined by the first intersection between $R_I(\varphi, \sigma)$ and $\mathcal{C}_M(I)$ from $\sigma = \varphi$ going down along $R_I(\varphi, \sigma)$. In Fig.5(b), we use a similar idea, but now, from $\sigma = \varphi$ going up along $R_I(\varphi, \sigma)$. Alternatively, if we choose τ^* with minimal absolute value, independently of going up or down, we obtain the scattering map plotted on Fig. 5(c). In this last case, there are orbits of the scattering maps that are not smooth in $\theta = \pi$. This happens because we change the homoclinic manifold Γ , so we are using, indeed, two different scattering maps. In [DS17] we chose scattering maps associated to a function τ^* with the minimal absolute value, which were called *primary* scattering maps. This example show us that is not enough to say what crest is associated to a scattering map, but it is also necessary to make explicit the criterion used for τ^* (going up or down along the NHIM lines, or choosing a minimal $|\tau^*|$).

The next lemma is a good example about the criteria for $\tau^*(I, \theta)$ and its consequences, and is used to prove Proposition 22. Before, a new notation is introduced. An *even* subindex k is assigned to the branches $\mathcal{C}_k(I)$ of $\mathcal{C}_M(I)$ when considering $\sigma, \varphi \in \mathbb{R}$

$$\xi_k(I, \varphi) = -\arcsin(\alpha(I)\mu \sin \varphi) + k\pi \quad \text{and} \quad \eta_k = -\arcsin\left(\frac{\sin \sigma}{\alpha(I)\mu}\right) + k\pi$$

and an *odd* subindex k to the branches $\mathcal{C}_k(I)$ of $\mathcal{C}_m(I)$ when considering $\sigma, \varphi \in \mathbb{R}$

$$\xi_k(I, \varphi) = \arcsin(\alpha(I)\mu \sin \varphi) + k\pi \quad \text{and} \quad \eta_k = \arcsin\left(\frac{\sin \sigma}{\alpha(I)\mu}\right) + k\pi.$$

We notice that the crests $\mathcal{C}(I)$ are naturally defined for $(\varphi, \sigma) \in \mathbb{T}^2$ and give rise to two different crests $\mathcal{C}_M(I)$, $\mathcal{C}_m(I)$ (except for the singular case $|\mu\alpha(I)| = 1$). When we run now over real values of φ, σ , we may have an *infinite* number of crests $\mathcal{C}_k(I)$, where even (odd) values of k are assigned to the branches of $\mathcal{C}_M(I)$ ($\mathcal{C}_m(I)$). Among them, we are going to use $\mathcal{C}_0(I)$, $\mathcal{C}_1(I)$ and $\mathcal{C}_2(I)$.

Lemma 20. *Let \mathcal{L}_0^* and \mathcal{L}_2^* be reduced Poincaré functions associated to the same crest $\mathcal{C}(I)$, where for \mathcal{L}_0^* we look at the first intersection points “under” $\sigma = \varphi$, that is, with $\mathcal{C}_0(I)$, and for \mathcal{L}_2^* we look at the first intersection points “over” $\sigma = \varphi$, that is, with $\mathcal{C}_2(I)$. Then we have*

$$\frac{\partial \mathcal{L}_0^*}{\partial \theta}(I, \theta) = -\frac{\partial \mathcal{L}_2^*}{\partial \theta}(I, 2\pi - \theta). \quad (30)$$

Remark 21. We say “under” $\sigma = \varphi$ and “over” $\sigma = \varphi$ for intersection points going down or up along $R_I(\varphi, \sigma)$, respectively on $(\varphi, \xi_0(I, \varphi))$ and $(\varphi, \xi_2(I, \varphi))$, because when the horizontal crest $\mathcal{C}_M(I)$ is defined for all $\varphi \in \mathbb{T}$ the graphs $(\varphi, \xi_0(I, \varphi))$ of $\mathcal{C}_0(I)$ and $(\varphi, \xi_2(I, \varphi))$ of $\mathcal{C}_2(I)$ are under and over the straight line $\sigma = \varphi$.

Proof. Let \mathcal{L}^* be a reduced Poincaré function (19)-(17), then

$$\frac{\partial \mathcal{L}^*}{\partial \theta}(I, \theta) = \frac{A_1(I) \sin(\theta - I\tau^*(I, \theta))}{I - 1}.$$

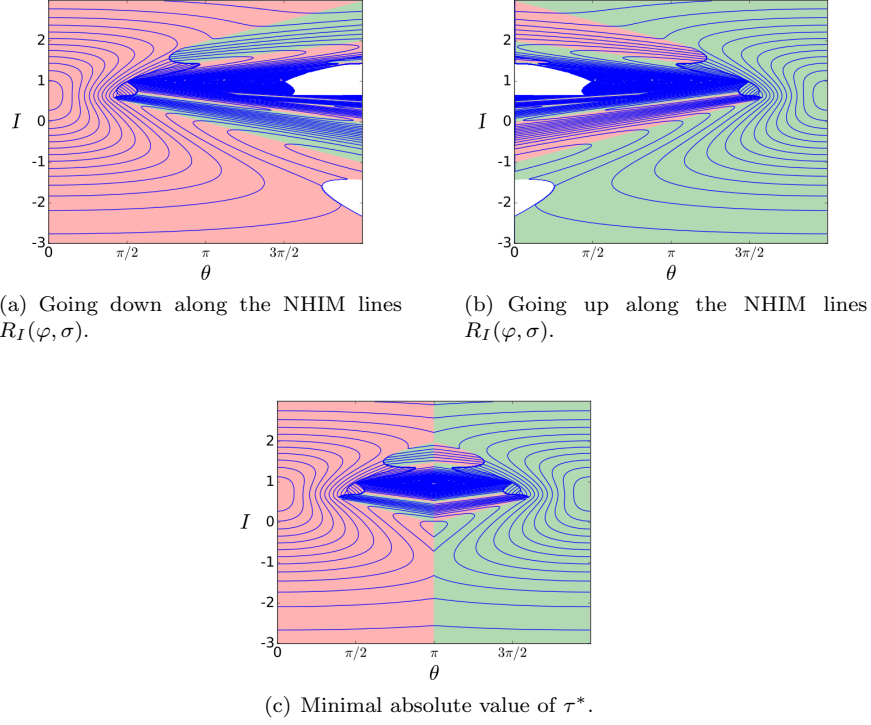


Fig. 5: Different phase space of scattering maps $\mathcal{S}(I, \theta)$ associated to the same horizontal crest $C_M(I)$, for $\mu = 0.6$ and $\varepsilon = 0.01$. The orbits of scattering maps are represented by the blue lines which are, up to $\mathcal{O}(\varepsilon^2)$, level sets of the reduced Poincaré function $\mathcal{L}^*(I, \theta)$. In the red zones the values of I on such orbits decrease, in the green one the values of I increase. The white regions are regions where $|\mu\alpha(I)\sin\varphi| > 1$ is satisfied.

So, equation (30) is satisfied if, and only if

$$\sin(\theta - I\tau_0^*(I, \theta)) = \sin(\theta - I(-\tau_2^*(I, 2\pi - \theta))). \quad (31)$$

We assume that the crest is horizontal and given by the graph of ξ_M , the other cases are analogous. Indeed, we are going to use

$$\xi_0(I, \varphi) = -\arcsin(\mu\alpha(I)\sin\varphi) \quad \text{and} \quad \xi_2(I, \varphi) = \xi_0(I, \varphi) + 2\pi. \quad (32)$$

This implies that the intersection point “under” $\sigma = \varphi$ is a point on the curve parameterized by $\xi_0(I, \varphi)$. Otherwise, the intersection “over” $\sigma = \varphi$ is a point on the curve parameterized by $\xi_2(I, \varphi)$. As the slope of the NHIM lines is $(I - 1)/I$, given a point (θ, θ) , we obtain

$$\frac{\xi_2(I, \theta - I\tau_2^*(I, \theta)) - \theta}{\theta - I\tau_2^*(I, \theta) - \theta} = \frac{I - 1}{I},$$

which can be rewritten as

$$\frac{2\pi + \xi_0(I, \theta - I\tau_2^*(I, \theta)) - \theta}{-I\tau_2^*(I, \theta)} = \frac{I - 1}{I}.$$

From this equation, we obtain an expression for $\tau_2^*(I, \theta)$

$$\tau_2^*(I, \theta) = \frac{-(2\pi + \xi_0(I, \theta - I\tau_2^*(I, \theta)) - \theta)}{I - 1}.$$

From the expressions of $\tau_2^*(I, \theta)$ above and (32),

$$\tau_2^*(I, 2\pi - \theta) = \frac{(\xi_0(I, \theta - I(-\tau_2^*(I, 2\pi - \theta))) + \theta)}{I - 1},$$

and therefore

$$\theta - (I - 1)(-\tau_2^*(I, 2\pi - \theta)) = \xi_0(I, \theta - (I - 1)(-\tau_2^*(I, 2\pi - \theta))),$$

which implies that $-\tau_2^*(I, 2\pi - \theta)$ is a time of intersection between the NHIM line and the curve parameterized by ξ_0 . In the case that there exists only one intersection point, this implies

$$\tau_0^*(I, \theta) = \tau_2^*(I, 2\pi - \theta).$$

So, condition (31) is satisfied. \square

Proposition 22. *Let $\mathcal{S}_1(I, \theta)$ be the scattering map associated to the graphs of ξ_1 and η_1 of $\mathcal{C}_1(I)$. Assuming $a_1, a_2 > 0$, for any I there exists a θ_+ such that $\dot{I} > 0$ for $\theta \in (\pi, \theta_+)$. Moreover, $\theta_+ \geq 3\pi/2$ for $I \notin (-1/2, 1/2)$.*

Proof. A proof is given in Appendix A. \square

Remark 23. If $a_1 < 0$, we have that there exists a θ_- such that $\dot{I} > 0$ for any $\theta \in (\theta_-, \pi)$.

Remark 24. An analogous proposition holds for $\mathcal{S}_2(I, \theta)$, the scattering map associated to the graphs of ξ_2 and η_2 of $\mathcal{C}_2(I)$. In such case, there is a θ_+ such that $\dot{I} \geq 0$ for any $\theta \in (\theta_+, 2\pi)$ where $\theta \geq 3\pi/2$ for $I \in (1/2, 3/2)$.

Note that this proposition leads us to ensure the diffusion in an analogous way to the one used to prove Theorem 4 in [DS17]. Next, the diffusion mechanism is stated and the Arnold diffusion is proven.

4 Arnold Diffusion

In this section we are going to complete our goal proving the existence of global instability or Arnold diffusion, that is, Theorem 1.

We begin by presenting some general geometrical properties of the scattering maps that we have to take into account to prove the theorem of diffusion. The first one reduces the study of scattering maps to positive values of μ . More precisely, we have the lemma below

Lemma 25. *The scattering map for a value of μ and $s = \pi$, associated to the intersection between $R(I, \varphi, s)$ and $C_m(I)$ ($C_M(I)$) has the same geometrical properties as the scattering map for $-\mu$ and $s = 0$, associated to the intersection between $R_\theta(I)$ and $C_M(I)$ ($C_m(I)$), i.e.,*

$$S_{m(M)}^\mu(I, \varphi, \pi) = S_{M(m)}^{-\mu}(I, \varphi, 0) = \mathcal{S}_{M(m)}^{-\mu}(I, \theta)$$

Proof. First, we look for τ_m^* such that the NHIM segment $R(I, \varphi, s)$ intersects the crest $C_m(I)$. If we fix $s = \pi$, we have from (17) and (18):

$$L_{\mu, m}^*(I, \varphi, \pi) = A_1(I) \cos(\varphi - I\tau_m^*(I, \varphi, \pi)) + A_2(I) \cos(\varphi - \pi - (I - 1)\tau_m^*(I, \varphi, \pi)). \quad (33)$$

Besides, τ_m^* satisfies

$$\mu\alpha(I) \sin(\varphi - I\tau_m^*) + \sin(\varphi - \pi - (I - 1)\tau_m^*) = 0,$$

or

$$-\mu\alpha(I) \sin(\varphi - I\tau_m^*) + \sin(\varphi - (I - 1)\tau_m^*) = 0.$$

We have that $\varphi - \pi - (I - 1)\tau_m^* \pmod{2\pi} = \xi_m(I, \varphi - I\tau_m^*)$ with $\pi/2 \leq \xi_m \leq 3\pi/2$. Then, for each τ_m^* there exists a $K \in \mathbb{Z}$ such that

$$\frac{\pi}{2} < \varphi - \pi - (I - 1)\tau_m^* + 2\pi K < \frac{3\pi}{2}.$$

This implies

$$\frac{3\pi}{2} < \varphi - (I-1)\tau_m^* + 2\pi K \quad \text{and} \quad \varphi - (I-1)\tau_m^* + 2\pi(K-1) < \frac{\pi}{2}.$$

Therefore,

$$\varphi - (I-1)\tau_m^* \pmod{2\pi} < \frac{\pi}{2} \quad \text{or} \quad \varphi - (I-1)\tau_m^* \pmod{2\pi} > \frac{3\pi}{2}.$$

We can conclude that $\varphi - (I-1)\tau_m^* \pmod{2\pi} = \xi_M(I, \varphi - I\tau_m^*)$. Therefore $\tau_m^*(I, \varphi, \pi)$ for μ is equal to $\tau_M^*(I, \varphi, 0)$ for $-\mu$. From (33), $L_{\mu, m}^*(I, \varphi, \pi)$ satisfies

$$\begin{aligned} L_{\mu, m}^*(I, \varphi, \pi) &= A_1(I) \cos(\varphi - \tau_M^*(I, \varphi, 0)) + (-A_2(I)) \cos(\varphi - (I-1)\tau_M^*(I, \varphi, 0)) \\ &= L_{-\mu, M}^*(I, \varphi, 0). \end{aligned}$$

Since $L_{\mu, m}^*(\cdot, \cdot, \pi)$ and $L_{-\mu, M}^*(\cdot, \cdot, 0)$ coincide, their derivatives too and this implies that

$$S_m^\mu(I, \varphi, \pi) = S_M^{-\mu}(I, \varphi, 0) = \mathcal{S}_M^{-\mu}(I, \theta).$$

□

From now on, just to simplify the exposition, a_1 and a_2 are considered positive. The same strategy used in [DS17] is applied to prove the existence the diffusion: we combine the scattering map in an interval of θ where $\dot{I} > 0$ and the inner map to build a diffusion pseudo-orbit. Then we apply shadowing results to get the existence of a diffusion orbit.

Since $I = 0$ and $I = 1$ are resonance values, the application of the inner map must be more careful, because in these resonance regions, for some orbits, the value of I decreases in order $\mathcal{O}(\sqrt{\varepsilon})$, i. e., the tori cannot be considered flat. We study the transversality between the foliations of invariant sets of the inner and the scattering map in resonant and non-resonant regions and its image under the scattering map \mathcal{S} . For more details and a more general case, the reader is referred to [DH09].

Consider the resonant region associated to $I = 0$. In such region, the tori can be approximated by $F^0(I, \varphi)$ given in (15). The transversality between invariant sets of the inner and the scattering map holds if the gradient vectors of the level curves of F^0 and \mathcal{L}^* are not parallel vectors, or equivalently,

$$\{F^0(I, \theta), \mathcal{L}^*(I, \theta)\} \neq 0,$$

where $\{, \}$ is the Poisson bracket,

$$\{F^0, \mathcal{L}^*\} = \frac{\partial F^0}{\partial \theta} \frac{\partial \mathcal{L}}{\partial I} - \frac{\partial F^0}{\partial I} \frac{\partial \mathcal{L}}{\partial \theta}.$$

From (15), the partial derivatives of F^0 are

$$\frac{\partial F^0}{\partial I} = I \quad \text{and} \quad \frac{\partial F^0}{\partial \theta} = -\varepsilon a_1 \sin \theta,$$

and since $\mathcal{L}^*(I, \theta) = A_1(I) \cos(\theta - I\tau^*(I, \theta)) + A_2(I) \cos(\theta - (I-1)\tau^*(I, \theta))$, we have the partial derivatives given by

$$\frac{\partial \mathcal{L}^*}{\partial \theta} = \frac{A_1(I) \sin(\theta - I\tau^*)}{I-1},$$

$$\frac{\partial \mathcal{L}^*}{\partial I} = A_1'(I) \cos(\theta - I\tau^*) + A_2'(I) \cos(\theta - (I-1)\tau^*) + A_1(I)\tau^* \sin(\theta - I\tau^*) + A_2(I)\tau^* \sin(\theta - (I-1)\tau^*).$$

Note that if $|I| > \mathcal{O}(\varepsilon)$, $\partial F^0/\partial I$ dominates $\partial F^0/\partial \theta$, so the Poisson bracket above can be reduced to

$$\{F^0, \mathcal{L}^*\} \simeq -\frac{\partial F^0}{\partial I} \frac{\partial \mathcal{L}}{\partial \theta} = \frac{-IA_1(I) \sin(\theta - I\tau^*)}{I-1}$$

Expanding $\sin(\theta - I\tau^*)$ in Taylor's series around $I = 0$, we have

$$\sin(\theta - I\tau^*) = \sin\theta + \mathcal{O}(I),$$

which implies $\{F^0, \mathcal{L}^*\} = 0$ if, and only if, $\theta \approx 0, \pi$, assuming that $\mathcal{O}(I)$ is small enough.

Now, we consider $I = \mathcal{O}(\varepsilon)$ and look at the intersections between the NHIM lines and the graph of ξ_1 . Note that as the value of I is close to 0 we can assume that the crests are horizontal. Using Taylor's series we can write

$$\begin{aligned} \sin(\theta - I\tau^*) &= \sin\theta + \mathcal{O}(I) & \cos(\theta - I\tau^*) &= \cos\theta + \mathcal{O}(I) \\ \sin(\theta - (I-1)\tau^*) &= \mathcal{O}(I) & \cos(\theta - (I-1)\tau^*) &= -1 + \mathcal{O}(I). \end{aligned}$$

This implies

$$\{F^0, \mathcal{L}^*\} = -\frac{IA_1(I)\sin\theta}{I-1} - \varepsilon a_1 \sin\theta (A'_1(I)\cos\theta - A'_2(I) + A_1(I)\tau^*\sin\theta) + \mathcal{O}(I^2, \varepsilon I). \quad (34)$$

Taylor expanding the functions $A_1(I)$, $A'_1(I)$ and $A'_2(I)$ around $I = 0$, we obtain

$$A_1(I) = 4a_1 + \mathcal{O}(I^2), \quad A'_1(I) = \mathcal{O}(I) \quad \text{and} \quad A'_2(I) = a_2\pi(\pi \coth \pi/2 - 2)\operatorname{csch}(\pi/2) + \mathcal{O}(I)$$

Plugging these expressions in (34), we set

$$\{F^0, \mathcal{L}^*\} = -\frac{4a_1 I \sin\theta}{I-1} - \varepsilon a_1 \sin\theta [a_2\pi(\pi \coth \pi/2 - 2)\operatorname{csch}(\pi/2) + 4a_1(\pi - \theta)\sin\theta] + \mathcal{O}(I^2, I\varepsilon).$$

So, $\{F^0, \mathcal{L}^*\} = 0 \Leftrightarrow a_1 \sin\theta \left[\frac{-4I}{I-1} - \varepsilon a_2\pi(\pi \coth \pi/2 - 2)\operatorname{csch}(\pi/2) + \varepsilon 4(\pi - \theta)\sin\theta \right] = 0$. In other words, we do not have transversality if, and only if, $\theta = 0, \pi$ or satisfies

$$(\pi - \theta)\sin\theta = \frac{I}{\varepsilon a_1} + \frac{\pi(\coth \pi/2 - 2)\operatorname{csch}(\pi/2)}{4},$$

which is not an horizontal curve in the plane (θ, I) and is transversal to an invariant torus of the inner dynamics.

For the other resonant region $I = 1$, F^1 is very similar. Assuming $I - 1 = \mathcal{O}(\varepsilon)$, we have

$$\{F^1, \mathcal{L}^*\} = a_2 \sin\theta \left\{ 4 \left(\frac{I-1}{I} \right) - \varepsilon [\pi a_1(2 - \pi \coth(\pi/2))\operatorname{csch}(\pi/2) + 4a_2 \sin\theta] \right\}.$$

Applying the same methodology, we obtain an analogous result for the other resonant region F^1 . In short, we conclude that the image $\mathcal{S}(\mathcal{T}_i)$ of an invariant torus \mathcal{T}_i of the inner map under the scattering map intersects transversally another invariant torus \mathcal{T}_{i+1} of the inner map.

Finally, in the non-resonant region, we notice that

$$\{F^{\text{nr}}, \mathcal{L}^*\} = -\frac{\partial F^{\text{nr}}}{\partial I} \frac{\partial \mathcal{L}^*}{\partial \theta} = -\frac{IA_1(I)\sin(\theta - I\tau^*)}{I-1},$$

just the same expression as the one for the resonance $I = 0$, so the transversality between invariant sets of the inner and the scattering map follows.

Now, a constructive proof of Theorem 1 is presented. This proof is similar to the proof presented in [DS17], but now, there is no any piece of ‘‘highway’’ or fast vertical lines where $|I|$ is large. So, the inner map is applied more times.

4.1 Proof of Theorem 1

Proof. First of all we have to choose what scattering map we use. This choice depends on the sign of μ as explained in Lemma 25. Assuming $\mu > 0$, we take $\mathcal{S}_1(I, \theta)$, the global scattering map associated to the graphs of ξ_1 and η_1 . If $a_1 > 0$, by Proposition 22 for any I there exists

an interval $\theta \in (\pi, \theta_+)$ where $\dot{I} > 0$. Define H_r the set $(\rho, \theta_+) \times [-I^*, I^*]$, where $\rho = \pi + \delta$ is such that $\pi < \rho < \theta_+$ and the transversality between NHIM lines and \mathcal{L}_1^* holds. We first construct a pseudo-orbit $\{(I_i, \theta_i) : i = 0, \dots, N_1\} \subset H_r$ with $I_0 = -I^*$ and θ_{N_1} as close as possible to ρ . Note that all these points lie in the same level curve of \mathcal{L}_1^* , that is, $\mathcal{L}_1^*(I_0, \theta_0) = \mathcal{L}_1^*(I_i, \theta_i)$, $i = 1, \dots, N_1$. Applying the inner dynamics, we get $(I_{N_1+1}, \theta_{N_1+1}) = \phi_{t_{N_1}}(I_{N_1}, \theta_{N_1})$ with $\theta_{N_1+1} \in (\rho, \theta_+)$ and then we construct a pseudo-orbit $\{(I_i, \theta_i) : i = N_1 + 1, \dots, N_1 + M_1\} \subset \mathcal{L}_1^*(I_{N_1+1}, \theta_{N_1+1}) = l_{N_1+1}$ with $\theta_i \in (\rho, \theta_{N_1+1})$, $\theta_+ - \theta_{N_1+M_1} = \mathcal{O}(\varepsilon^2)$. Applying the inner dynamics, we get $(I_{N_1+M_1+1}, \theta_{N_1+M_1+1}) = \phi_{t_{N_1+M_1}}(I_{N_1+M_1}, \theta_{N_1+M_1})$ with $\theta_{N_1+M_1+1} \in (\rho, \theta_+)$. Recursively, we construct a pseudo-orbit $\{(I_i, \theta_i) : i = N_1 + 1, \dots, N_2\}$ such that $I_{N_2} \geq I^*$. In the same ways as in [DS17] (Theorem 4), we can apply shadowing techniques of [FM00, FM03, GLS14], due to the fact that the inner dynamics is simple enough to satisfy the required hypothesis of these references, to prove the existence of a diffusion trajectory. If $a_{10} < 0$, changing H_r to $H_l = (\theta_+, \pi)$ all the previous reasoning applies. \square

Remark 26. Considering Remark 4, Remark 9, Remark 12 and Remark 16, for any $r \in (0, 1)$, an equivalent diffusion result is readily obtained.

5 Piecewise smooth global scattering maps

In this section, the geometric freedom of the choice of τ^* is explored. Until now, only two different scattering maps have been used to build a global one, and this was enough to ensure diffusion. But, with this approach, finding a diffusion pseudo-orbit is not always easy enough and this pseudo-orbit can be also complicated. This depends simply on the “aspect” of the scattering map obtained.

We now suggest a new criterion to choose τ^* : to take the minimal value for $|\tau^*|$ for any (θ, I) . This provides us with a piecewise smooth global scattering map with a good property: the phase space of this scattering map which is $\mathcal{O}(\varepsilon^2)$ -close to the level sets of the reduced Poincaré function $\mathcal{L}^*(I, \theta)$ associated to the chosen τ^* is simpler and “cleaner” than the phase spaces of other scattering maps displayed up to now. By a cleaner scattering map, we mean that we can easily identify and understand the orbits of the scattering maps, except for a small region which contains the tangency locus.

Besides, the zones where the value of I is increased or decreased under the scattering map is well behaved. I decreases for $\theta \in (0, \pi)$ (the red region on all pictures in Fig. 6) and I increases for $\theta \in (\pi, 2\pi)$ (the green region on all pictures in Fig. 6). So it is easy to infer that for finding a diffusion pseudo-orbit it is enough to build a combination between the inner map and this scattering map restricted to $(\pi, 2\pi)$, for example if an increased value of I is wished. The same idea used in the proof of Theorem 1.

Observe that the scattering maps we are now considering are a mix of the scattering maps studied previously. As an example, we illustrate the scattering map obtained for $\mu = 0.9$. Such scattering map can be divided into three regions and in each region, the scattering map coincides with a scattering map studied before.

In Fig. 7, for regions I ($0 < \theta < \pi/2$), II ($\pi/2 < \theta < 3\pi/2$) and III ($3\pi/2 < \theta < 2\pi$) the scattering map has the following correspondence:

- I Extended scattering map $\mathcal{S}_0(I, \theta)$ associated to the horizontal $\mathcal{C}_M(I)$ “under” $\sigma = \varphi$.
- II Extended scattering map $\mathcal{S}_1(I, \theta)$ associated to the horizontal $\mathcal{C}_m(I)$.
- III Extended scattering map $\mathcal{S}_2(I, \theta)$ associated to the horizontal $\mathcal{C}_M(I)$ “over” $\sigma = \varphi$.

If extended scattering maps are not considered and we just use scattering maps associated to horizontal and vertical crests, one can see that these scattering maps can be divided into 6 regions, i.e., they can be viewed as a combination of up to 6 scattering maps.

Another property of these scattering maps is the loss of differentiability on the straight lines $\theta = \pi/2$ and $\theta = 3\pi/2$. The vector field associated to the Hamiltonian $-\mathcal{L}_i^*$ defined around these

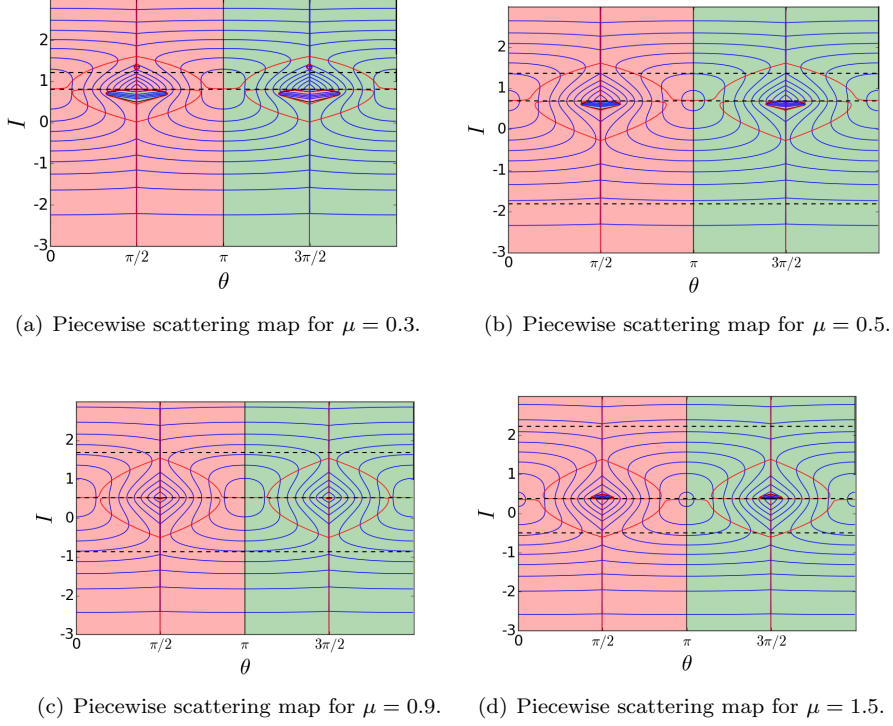


Fig. 6: Examples of piecewise smooth global scattering maps. The orbits of scattering maps are represented by the blue lines. In the red zones the values of I on such orbits decrease, in the green one the values of I increase.

discontinuity lines behaves as the vector fields studied in non-smooth dynamics theory. More precisely, we can find regions with slide and unstable slide behavior [Fil88]. In a future work, we envisage to design special pseudo-orbits along these discontinuity lines using such theory. Note that these pseudo-orbits would be very similar to the “highways” defined in [DS17], so in principle, one can expect fast and simple diffusion along these discontinuity lines.

Acknowledgments

The authors would like to express their gratitude to the anonymous referees for their comments and suggestions which have contributed to improved the final form of this paper. We also thank C. Simó for several discussions and comments.

A Proof of Proposition 22

Proposition 22. *Let $\mathcal{S}_1(I, \theta)$ be the scattering map associated to the graphs ξ_1 and η_1 . Assuming $a_1, a_2 > 0$, then for any I , there exists a θ_+ such that $\dot{I} > 0$ for $\theta \in (\pi, \theta_+)$. Moreover, $\theta_+ \geq 3\pi/2$ for $I \notin (-1/2, 1/2)$.*

Proof. We have

$$\dot{I} = \frac{\partial \mathcal{L}^*}{\partial \theta}(I, \theta) = \frac{A_1(I) \sin(\theta - I\tau^*(I, \theta))}{I - 1} = -\frac{A_2(I) \sin(\theta - (I - 1)\tau^*(I, \theta))}{I}. \quad (35)$$

where $A_1(I)$ and $A_2(I)$ are positive, because $a_1, a_2 > 0$. Notice that $\mu = a_1/a_2 > 0$.

Note that as $(I, \varphi = \pi, \theta = \pi)$ is always on the crest $\mathcal{C}_m(I)$, $\tau^*(I, \pi) = 0$ for all I .

Consider first the case of horizontal crests ($|\alpha(I)\mu| < 1$).

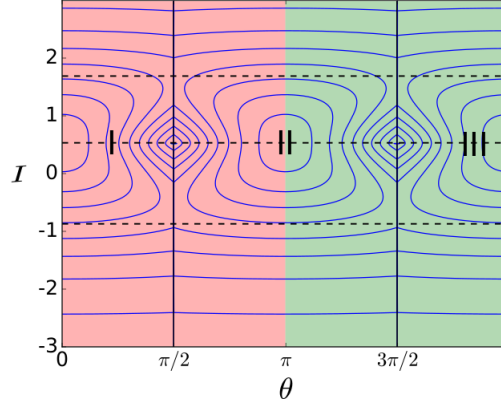


Fig. 7: A piecewise smooth global scattering map divided into 3 regions. The vertical black lines are the boundaries of the domains of smooth scattering maps.

- a) For $I < 0$, the function $\alpha(I)$ introduced in (26) satisfies $\alpha(I) > 0$, and from (27), $\sin(\xi_1(I, \varphi)) \sin \varphi = -\mu\alpha(I) \sin \varphi \leq 0$. Take $\theta = \frac{3\pi}{2}$; since $I < 0$, the slope $m = (I - 1)/I$ of the NHIM lines is greater than 1. Therefore, $3\pi/2 - I\tau_1^*(I, 3\pi/2) \in (\pi, 3\pi/2)$. This implies that for any $\theta \in (\pi, 3\pi/2)$, $\theta - I\tau_1^*(I, \theta) \in (\pi, 3\pi/2)$, so $\sin(\theta - I\tau_1^*) < 0$. From (35), $\dot{I} > 0$.
- b) For $0 < I < 1$, $\alpha(I) < 0$, so $\sin \xi_1(I, \varphi) \sin \varphi \geq 0$. Besides, $m < 0$, so if we look for θ_* satisfying

$$\begin{aligned} \theta - I\tau &= 2\pi \\ \theta - (I - 1)\tau &= \pi, \end{aligned} \quad (36)$$

we have that for any $\theta \in (\pi, \theta_*)$, $\theta - I\tau_1^* \in (\pi, 2\pi)$. By solving (36) and defining $\theta_+ := \theta_*$, we obtain $\theta_+ = (2 - I)\pi$. Then, $\sin(\theta - I\tau_1^*(I, \theta)) < 0$ and therefore $\dot{I} > 0$ for any $\theta \in (\pi, \theta_+ = (2 - I)\pi)$. In particular, $\theta_+ < 3\pi/2$ if, and only if, $I \in (1/2, 1)$.

- c) For $I > 1$, one more time $\alpha(I) > 0$ and $\sin \xi_1(I, \varphi) \sin(\varphi) < 0$, but now $0 < m = 1 - 1/I < 1$. We first fix $\theta = 3\pi/2$ and search for I such that

$$\begin{aligned} \frac{3\pi}{2} - I\tau^*(I, 3\pi/2) &= 0 \\ \frac{3\pi}{2} - (I - 1)\tau^*(I, 3\pi/2) &= \pi. \end{aligned}$$

We obtain $I = 3/2$, so $\theta - I\tau_1^*(I, \theta) \in (0, \pi)$ for any $I \geq 3/2$ and $\theta \in (\pi, \theta_+ = 3\pi/2)$. Consequently, $\sin(\theta - I\tau_1^*(I, \theta)) > 0$ and $\dot{I} > 0$. For the values of $I \in (1, 3/2)$ we change the strategy. We look for θ_* such that

$$\begin{aligned} \theta - I\tau^*(I, \theta) &= 0 \\ \theta - (I - 1)\tau^*(I, \theta) &= \pi. \end{aligned}$$

We have $\theta_* = \pi I$ and $\theta - I\tau_1^*(I, \theta_*) \in (0, \pi)$ for any $I \in (1, 3/2)$ and $\theta \in (\pi, \theta_*)$, so $\dot{I} > 0$. Note that $\theta_* < 3\pi/2$ and we can define $\theta_+ := \theta_*$.

Observe that for $I = 1$ the crests are vertical, and for $I = 0$, $\theta = \theta - I\tau_1^*(I, \theta)$, and $\dot{I} > 0$ for $\theta \in (\pi, 3\pi/2)$.

Consider now the case of vertical crests ($|\alpha(I)\mu| > 1$).

- a) For $I < 0$, $\sin \eta_1(I, \sigma) \sin \sigma = -\mu\alpha(I) \sin^2 \sigma \leq 0$ and $m > 1$. We fix $\theta = 3\pi/2$ and look for I such that

$$\begin{aligned} 3\pi/2\pi - I\tau^* &= \pi \\ 3\pi/2 - (I-1)\tau^*(I, 3\pi/2) &= 0. \end{aligned}$$

We obtain $I = -1/2$ and therefore, $\sin(\theta - (I-1)\tau_1^*(I, \theta)) > 0$ for $I \in (-\infty, -1/2)$ and $\theta \in (\pi, 3\pi/2)$. Consequently, $\dot{I} > 0$ from (35). For $I \in (-1/2, 0)$, we have that $\theta_+ = (1-I)\pi$ satisfies

$$\begin{aligned} \theta - I\tau^*(I, \theta_+) &= \pi \\ \theta_+ - (I-1)\tau^*(I, \theta_+) &= 0. \end{aligned}$$

Therefore, $\sin(\theta - (I-1)\tau_1^*(I, \theta)) > 0$ and $\dot{I} > 0$ for any $\theta \in (\pi, \theta_+)$.

- b) For $0 < I < 1$ $\sin \eta_1(I, \sigma) \sin \sigma \geq 0$ and $m < 0$. $\theta_+ = (I+1)\pi$ satisfies

$$\begin{aligned} \theta - I\tau^*(I, \theta_+) &= \pi \\ \theta_+ - (I-1)\tau^*(I, \theta_+) &= 2\pi. \end{aligned}$$

So, $\sin(\theta - (I-1)\tau_1^*(I, \theta)) > 0$ and $\dot{I} > 0$ for any $\theta \in (\pi, \theta_+)$. Note that $\theta_+ < 3\pi/2$ for $I \in (0, 1/2)$.

- c) Finally, for $I > 1$, $\sin \eta_1(I, \sigma) \sin \sigma \leq 0$. We have that $\theta - (I-1)\tau_1^*(I, \theta) \in (\pi, 2\pi)$, so $\sin(\theta - (I-1)\tau_1^*(I, \theta)) < 0$ and $\dot{I} > 0$ for any $\theta \in (\pi, 3\pi/2)$.

For $I = 0$ the crests are horizontal. For $I = 1$, $\theta = \theta - (I-1)\tau_1^*(I, \theta)$, so $\dot{I} > 0$ for $\theta \in (\pi, 2\pi)$. \square

References

- [CDMR06] E. Canalias, A. Delshams, J. J. Masdemont and P. Roldan. The scattering map in the planar restricted three body problem. *Celestial Mechanics and Dynamical Astronomy*, 95(1):155–171, May 2006.
- [CG94] L. Chierchia and G. Gallavotti. Drift and diffusion in phase space. *Ann. Inst. H. Poincaré Phys. Théor.*, 60(1):144, 1994.
- [CGL16] M. J. Capinski, M. Gidea and R. de la Llave. Arnold diffusion in the planar elliptic restricted three-body problem: mechanism and numerical verification. *Nonlinearity*, 30(1):329, 2016.
- [Che17] C.-Q. Cheng. Dynamics around the double resonance. *Camb. J. Math.*, 5(2):153–228, 2017.
- [DGR13] A. Delshams, M. Gidea and P. Roldán. Transition map and shadowing lemma for normally hyperbolic invariant manifolds. *Discrete & Continuous Dynamical Systems - A*, 33(1078-0947 2013 3 1089):1089, 2013.
- [DGR16] A. Delshams, M. Gidea and P. Roldan. Arnold’s mechanism of diffusion in the spatial circular restricted three-body problem: A semi-analytical argument. *Physica D: Nonlinear Phenomena*, 334(Supplement C):29 – 48, 2016. Topology in Dynamics, Differential Equations, and Data.
- [DH09] A. Delshams and G. Huguet. Geography of resonances and Arnold diffusion in a priori unstable Hamiltonian systems. *Nonlinearity*, 22(8):1997–2077, 2009.

- [DH11] A. Delshams and G. Huguet. A geometric mechanism of diffusion: rigorous verification in a priori unstable Hamiltonian systems. *J. Differential Equations*, 250(5):2601–2623, 2011.
- [DLS00] A. Delshams, R. de la Llave and T. M. Seara. A geometric approach to the existence of orbits with unbounded energy in generic periodic perturbations by a potential of generic geodesic flows of \mathbf{T}^2 . *Comm. Math. Phys.*, 209(2):353–392, 2000.
- [DLS06] A. Delshams, R. de la Llave and T. M. Seara. A geometric mechanism for diffusion in Hamiltonian systems overcoming the large gap problem: heuristics and rigorous verification on a model. *Mem. Amer. Math. Soc.*, 179(844):viii+141, 2006.
- [DLS08] A. Delshams, R. de la Llave and T. M. Seara. Geometric properties of the scattering map of a normally hyperbolic invariant manifold. *Adv. Math.*, 217(3):1096–1153, 2008.
- [DMR08] A. Delshams, J. J. Masdemont and P. Roldán. Computing the scattering map in the spatial hill’s problem. *Discrete & Continuous Dynamical Systems - B*, 10(1531-3492 2008 2/3, September 455):455, 2008.
- [DS97] A. Delshams and T. M. Seara. Splitting of separatrices in Hamiltonian systems with one and a half degrees of freedom. *Math. Phys. Electron. J.*, 3:Paper 4, 40, 1997.
- [DS17] A. Delshams and R. G. Schaefer. Arnold diffusion for a complete family of perturbations. *Regular and Chaotic Dynamics*, 22(1):78–108, 2017.
- [DT16] M. N. Davletshin and D. V. Treschev. Arnold diffusion in a neighborhood of strong resonances. *Proc. Steklov Inst. Math.*, 295(1):63–94, 2016.
- [Fil88] A. F. Filippov. *Differential equations with discontinuous righthand sides*, volume 18 of *Mathematics and its Applications (Soviet Series)*. Kluwer Academic Publishers Group, Dordrecht, 1988. ISBN 90-277-2699-X. Translated from the Russian.
- [FM00] E. Fontich and P. Martín. Differentiable invariant manifolds for partially hyperbolic tori and a lambda lemma. *Nonlinearity*, 13(5):1561–1593, 2000.
- [FM03] E. Fontich and P. Martín. Hamiltonian systems with orbits covering densely submanifolds of small codimension. *Nonlinear Anal.*, 52(1):315–327, 2003.
- [GLS14] M. Gidea, R. de la Llave and T. M. Seara. A general mechanism of diffusion in Hamiltonian systems: Qualitative results, 2014. Preprint, arXiv:1405.0866.
- [GM17] M. Gidea and J.-P. Marco. Diffusion along chains of normally hyperbolic cylinders, 2017. Preprint, arXiv:1708.08314.
- [GT17] V. Gelfreich and D. Turaev. Arnold diffusion in a priori chaotic hamiltonian systems. *Comm. Math. Phys.*, pages 507–547, 2017.
- [LMS16] L. Lazzarini, J.-P. Marco and D. Sauzin. Measure and capacity of wandering domains in gevrey near-integrable exact symplectic systems, 2016. Preprint, arXiv:1507.02050. To appear in *Mem. Amer. Math. Soc.*
- [Mar16] J.-P. Marco. Arnold diffusion for cusp-generic nearly integrable convex systems on \mathbb{A}^3 , 2016. Preprint, arXiv:1602.02403.